DOI: 10.18462/iir. 10.18462/iir.icr.2023.0045

Adaptive model-based monitoring of large-scale heat pump prone to evaporator fouling

José Joaquín AGUILERA*[(a)], Wiebke MEESENBURG[(a)], Wiebke Brix MARKUSSEN[(b)] , Jonas Lundsted POULSEN [(b)] , Benjamin ZÜHLSDORF[(b)], Brian ELMEGAARD[(a)]

[(a)] Section of Thermal Energy, Department of Civil and Mechanical Engineering, Technical University of Denmark, DK-2800, Kgs. Lyngby, Denmark

[(b)] Danish Technological Institute, DK-8000, Aarhus, Denmark

*Corresponding author: jojap@dtu.dk

ABSTRACT

Widespread implementation of large-scale heat pumps can reduce carbon emissions from district heating systems. Fouling of heat exchangers is a common fault in such heat pumps, affecting their performance and availability. A monitoring framework was developed and tested in a heat pump prone to evaporator fouling. Here, a dynamic simulation model was calibrated based on data retrieved from existing control and supervision systems through cloud-based data acquisition. The effects of fouling on the evaporator thermal resistance, and thereby on the system performance, resulted to be larger than the effects on the source side pressure drop. The inclusion of those effects in the model calibration reduced the simulation errors by up to 12 % points compared to an initial calibration. The framework allowed the assessment of the effectiveness of a cleaning-in-place procedure. This also enabled to evaluate cleaning-in-place usage for periods when the heat pump was most affected by fouling.

Keywords: heat pump, district heating, fouling, operation monitoring, digital twin

1. INTRODUCTION

Electricity-driven heat pumps (HPs) are one of the most promising technologies to decarbonize European district heating systems by the use of available renewable energy sources and the recovery of industrial excess heat (Kosmadakis, 2019). Countries like Austria, Denmark, Finland, and Sweden already defined targets to decarbonize their district heating networks, where HPs are set to play a major role (IEA, 2022). In particular, about a third of the heat supplied in Danish district heating systems is expected to come from HPs by 2030 (Danish Energy Agency, 2022).

Evaporator fouling is among the most common faults in large-scale HPs (i.e. systems with heat capacities over 200 kW (Pieper et al., 2018)), as indicated in Aguilera et al. (2022b). Fouling leads to an increase of the thermal resistance and pressure drop in heat exchangers (HXs). This can affect the performance and availability of HPs, particularly when they need to be shut-down to be serviced. Mitigation strategies for fouling include cleaning-in-place (CIP) methods, which enable the removal of material deposition in HXs without disassembly. However, it is a challenge to determine the effectiveness of CIP methods when direct observations of the fouled surfaces are not available.

Suitable monitoring strategies in large-scale HPs may contribute to the reduction of downtime periods as well as degradation of component and system performance. Common monitoring technologies for large-scale HPs include supervisory control and data acquisition (SCADA) systems, where HP operators are informed about a number of measured and control variables.

Digital twins are virtual representations of physical processes and systems, which include numerical models that can adapt their structure based on operational data from the system they describe. This enables an accurate representation of a system's operation over time, where performance degradation of components and faults may occur. However, the implementation of digital twins for HPs remains limited, where a few application examples are found in the literature such as those from Seifert et al., 2022 and Vering et al., 2021.

The objective of this study was to develop and test an online model-based monitoring framework regarded as a digital twin for the analysis of the performance and faulty operation of a large-scale HP susceptible to evaporator fouling.

2. METHOD

This section provides a description of a large-scale HP system used as case study and the development of a model-based monitoring framework that was tested in such a system.

2.1. System description

The HP used as case study was a two-stage ammonia system with open intercooler (shown in Figure 1), located in Copenhagen, Denmark. This study focuses on one of the two identical 2-MW HPs connected in parallel to the same source and sink streams. This system recovered heat from industrial wastewater at approximately 23 ˚C from a biochemical plant and delivered heat at around 68 ˚C to a local district heating network. Each HP was an off-the-shelf unit that included two electronic expansion valves, one reciprocating compressor for each of the two stages and an open intercooler between them. All HXs were shell-and-plate with corrugated plates. A desuperheater, condenser, receiver and subcooler were embedded in the same component.

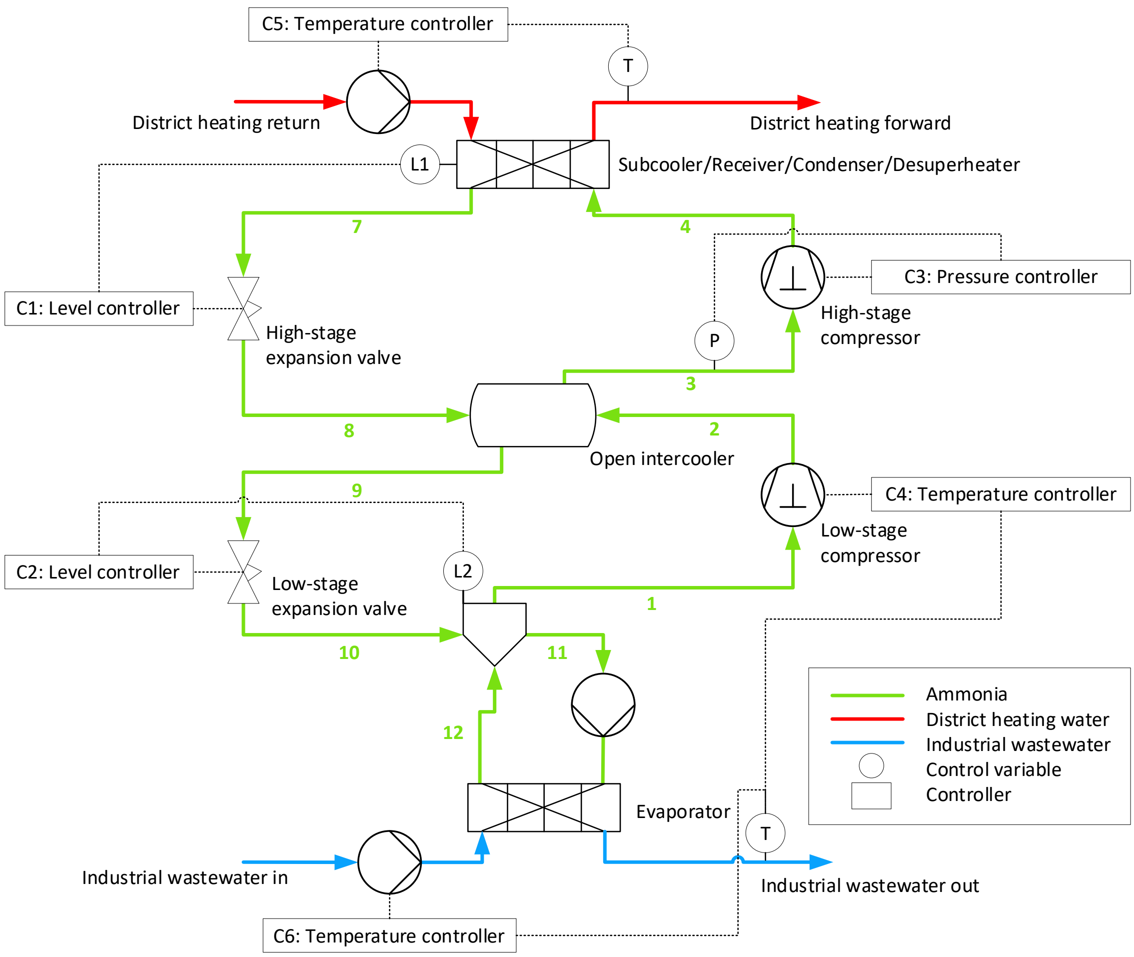

Figure 1: PI diagram of the HP analysed in the present study.

The operator of the HP described that its operation was frequently affected by fouling in the source stream, where calcium compounds and organic elements originated from an open cooling tower and biochemical industrial processes deposited on the evaporator heat transfer surface. A CIP procedure was performed when a significant decrease in performance and/or capacity of the system occurred. The CIP process consisted of the circulation of an acid solution to remove inorganic materials and a basic solution for organic materials by means of a flushing system. The HP was not in operation when the CIP was applied.

2.2. Dynamic simulation model

A simulation model of the HP was developed in the programming language Modelica integrated in the software Dymola (Dassault Systèmes, 2022), where the TIL Suite library (TLK-Thermo GmbH, 2023) was used. The compressor models corresponded to the reciprocating compressor models from the TIL Suite library. The shell-and-plate HXs were represented by plate HX models from the same library. This simplification was also applied in a related study from Meesenburg et al. (2019), where the outputs from the simulation model corresponded with the measurements. The pressure drop through all HXs was neglected, except from the pressure drop on the evaporator source side, which was determined from measured data after the CIP was applied (i.e. low fouling conditions). Expansion valves, vessels, pumps, sensors and controllers in the system were also represented by available models in the TIL Suite library. Heat losses to the environment were neglected for all the components in the model as well as the presence of oil in the HP. The HP model was converted into a functional mockup unit (FMU) and simulated in Python by means of the FMPy module (Sommer et al., 2023). This was a useful approach to perform multiple simulations and integrate them in the optimization routines required for model calibration. The model inputs were the volumetric flow rate of the source and sink streams ($\dot{V}_{\mathrm{source}}$ and $\dot{V}_{\mathrm{sink}}$, respectively), the inlet temperatures from the source and sink streams ($T_{\mathrm{source,in}}$ and $T_{\mathrm{sink,in}}$, respectively) and the intermediate pressure and source outlet temperature set points ($p_{\mathrm{m,SP}}$ and $T_{\mathrm{source,SP}}$, respectively). These set points were used for the high-stage (HS) and low-stage (LS) compressor controllers. All inputs were directly determined from measurements, except for the $p_{\mathrm{m,SP}}$ that was not available and was estimated as the arithmetic mean of the intermediate pressure over a period of one day.

2.3. Monitoring framework

The HP was provided with a cloud data management system, which retrieved operational data from a SCADA system. Operational data from sensing devices and actuators were collected in real-time from the system controller, stored in a database server, and made accessible through a web application programming interface (API). This data included temperature and volume flow rate measurements of the secondary streams, refrigerant state measurements in the suction and discharge lines of the compressors and the condenser, as well as compressor and pump current measurements.

The monitoring framework shown in Figure 2, described in detail in the following sub-sections, was comprised of a moving window approach, where one period (or window) was processed at a time. First, a batch of data representing the last 12 hours of operation was retrieved from the API and processed in Python. The user was able to define whether the latest operational window or an older one was used for the initial model calibration, or IMC. In the present study, the operational window for the IMC was right after the CIP was applied. This enabled to calibrate the model on a period where the effects of fouling over the HP were minimal. A sensitivity analysis was used for the selection of model parameters adjusted in the IMC. Afterwards, the thermal resistance ($R_{\mathrm{th,f}}$) and pressure drop related to fouling ($\mathrm{d}p_{\mathrm{f}}$) were calibrated in a process called fouling calibration (FC), where four different operational windows were used . Finally, the calibrated model was simulated for the operational windows right after those used in the FC in a process named fouling analysis (FA). Here, the current and historical effects of fouling on the HP were compared.

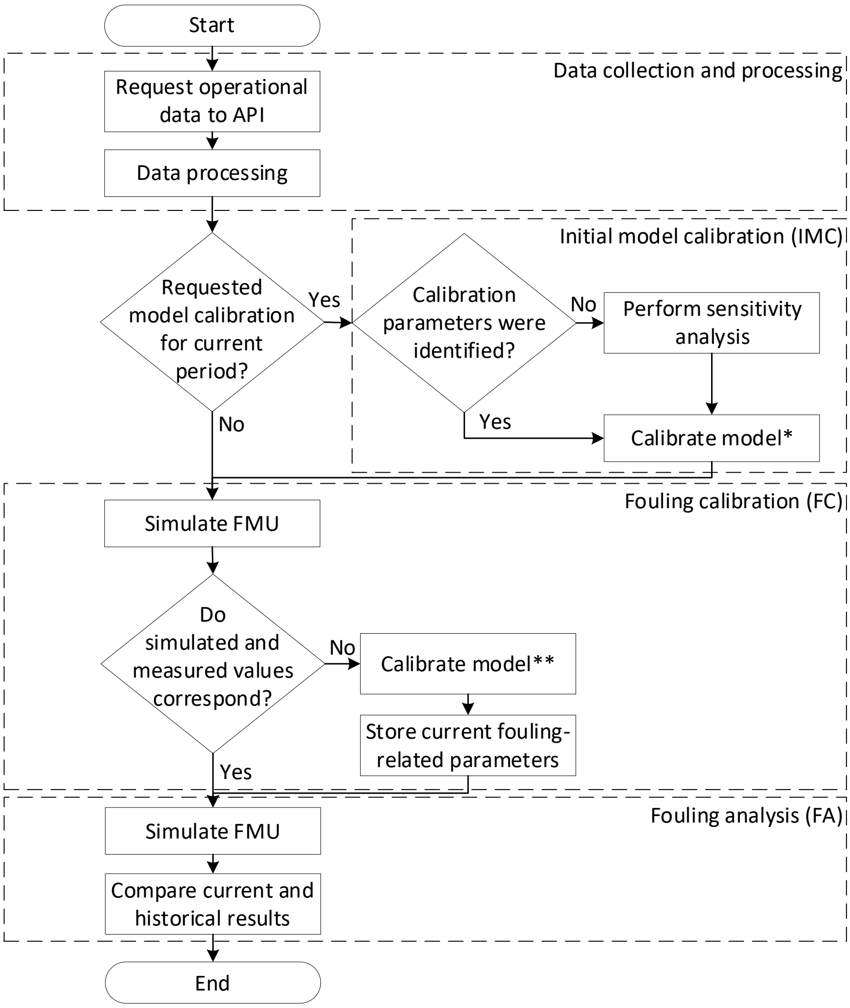

Figure 2: Flow diagram of the proposed framework. (*) Adjustment of time-invariant geometry- and control-related parameters. (**) Adjustment of time-dependent fouling-related parameters.

2.3.1. Data processing

Operational data from the HP was used to perform energy and mass balance calculations of the main system components (i.e. compressors, HXs, vessels and expansion valves) using Python. Here, refrigerant state calculations were done with the Coolprop database (Bell et al., 2014). The heat output ($\dot{Q}_h$) and the coefficient of performance (COP) of the HP were determined with the sink stream inlet and outlet temperatures ($T_{sink,in}$ and $T_{sink,out}$, respectively), the mass flow rate ($\dot{m}_{sink}$) and the specific heat capacity of water ($c_{p,w}$), as seen in Eq. 1 and Eq. 2 .

$$\dot{Q}_{\mathrm{h}} = C_{\mathrm{p,w}} \cdot \dot{m}_{\mathrm{sink}} \cdot (T_{\mathrm{sink,out}} - T_{\mathrm{sink,in}}) \qquad \text{Eq. (1)}$$

$$\mathrm{COP} = \dot{Q}_{\mathrm{h}} \cdot \dot{W}_{\mathrm{total}}^{\ -1} \qquad \text{Eq. (2)}$$

The effect of fouling on the heat transferred in the evaporator was determined through its UA-value with Eq. 3 and Eq. 4, whereas the effect on the source stream pressure drop was estimated through Eq. 5. This required the mass flow of water in the evaporator ($\dot{m}_{source}$), the water inlet and outlet temperatures ($T_{sink,in}$ and $T_{sink,out}$, respectively) and the ammonia evaporation temperature (T_e). The calculations considered the evaporator before and after the CIP was applied, i.e. under actual ($R_{th,eva}$, dp_{eva}) and clean conditions ($R_{th,eva,clean}$, $dp_{eva,clean}$), respectively. Here, the relationship between the source stream mass flow rate and pressure drop in the evaporator under clean conditions was found by fitting a quadratic regression model.

$$UA_{\mathrm{eva}} = C_{\mathrm{p,w}} \cdot \dot{m}_{\mathrm{source}} \cdot \ln((T_{\mathrm{source,in}} - T_{\mathrm{e}}) \cdot (T_{\mathrm{source,out}} - T_{\mathrm{e}})^{-1}) \qquad \text{Eq. (3)}$$

$$R_{\mathrm{th,f}} = \mathrm{UA_{eva}}^{-1} - \mathrm{UA_{eva,clean}}^{-1} = R_{\mathrm{th,eva}} - R_{\mathrm{th,eva,clean}} \quad \text{Eq. (4)}$$

$$dp_{\mathrm{f}} = dp_{\mathrm{eva}} - dp_{\mathrm{eva,clean}} \quad \text{Eq. (5)}$$

2.3.2. Calibration process

The Python modules AixCaliBuHA (Wüllhorst et al., 2022) and Pymoo (Blank and Deb, 2020) were used for model calibration and SALib (Herman and Usher, 2017) for sensitivity analysis. The parameters shown in Table 1 were used for the IMC and FC, and were assumed to be uniformly distributed within the ranges specified in the table. The final selection of the parameters for the IMC was done through the Morris and Sobol methods for sensitivity analysis. The total effect index (S_T) was used in the Sobol method, which enables the identification of the remaining variance of model outputs when a parameter is defined constant. The S_T highlighted the overall influence of a parameter on certain outputs of interest for calibration, called calibration targets (CTs). In the Morris method, the absolute mean value of the elementary effects of each parameter (μ^*) on the CTs was calculated. This corresponded to the ratio of the variation of the CTs to the variation of a parameter.

Table 1: List of parameters pre-selected for the IMC and selected for the FC.

Calibration process	Parameter	Component	Description	Variation range
IMC	CF_{SC}	Subcooler	Heat transfer area correction factor	0.5 to 1.5 [-]
	Φ_{SC}		Chevron angle	30 to 60 [°]
	CF_{con}	Condenser	Heat transfer area correction factor	0.5 to 1.5 [-]
	Φ_{con}		Chevron angle	30 to 60 [°]
	CF_{DSH}	DSH	Heat transfer area correction factor	0.5 to 1.5 [-]
	Φ_{DSH}		Chevron angle	30 to 60 [°]
	CF_{eva}	Evaporator	Heat transfer area correction factor	0.5 to 1.5 [-]
	Φ_{eva}		Chevron angle	30 to 60 [°]
	$Ti_{com,HS}$	HS compressor	Time constant in PI controller	10 to 2000 [s]
	$Ti_{val,HS}$	HS expansion valve	Time constant in PI controller	10 to 2000 [s]
	$Ti_{com,LS}$	LS compressor	Time constant in PI controller	10 to 2000 [s]
	$Ti_{val,HS}$	LS expansion valve	Time constant in PI controller	10 to 2000 [s]
FC	$R_{th,f}$	Evaporator	Fouling-related thermal resistance	0 to 0.02 [K/kW]
	dp_f	Evaporator	Fouling-related pressure drop	0 to 0.5 [Bar]

The IMC incorporated time-invariant geometry- and control-related parameters. Here, the calibration of the time constants from the PI controllers allowed the adjustment of the dynamics of the model to those from the physical HP. The calibration of the proportional constants of the PI controllers was attempted, but in the end, they were determined by the method from (Ziegler and Nichols, 1942), which proved to be simpler and effective.

The optimization problem consisted of the adjustment of the parameters selected for calibration such that the normalized root mean square error (NRMSE) between measured and simulated CTs was minimized, as described in Eq. 6 and Eq. 7. This was done for the 12-hour operational windows with n equal to 720 data points retrieved with a one-minute interval. For the IMC, the CTs were the $T_{\mathrm{sink,out}}$, $\dot{W}_{\mathrm{total}}$ and the evaporation pressure (p_e) with weights (w_i) equal to 25 %, 50 % and 25 %, respectively. The CTs for the FC process corresponded to the p_e and the total pressure drop in the evaporator source stream (dp_{eva}), both with equal weights of 50 %. The weights used for IMC and FC were determined heuristically.

$$\min\left(\textstyle\sum_{i=1}^{n} w_i \cdot \mathrm{NRMSE}(\mathrm{CT}_{meas}, \mathrm{CT}_{sim})\right) \quad \text{Eq. (6)}$$

$$\mathrm{NRMSE}(\mathrm{CT}_{meas}, \mathrm{CT}_{sim}) = \overline{\mathrm{CT}}_{meas}^{\,-1} \cdot \sqrt{n^{-1} \cdot \textstyle\sum_{i=1}^{n} (\mathrm{CT}_{sim,i} - \mathrm{CT}_{meas,i})^2} \quad \text{Eq. (7)}$$

The optimization problem for calibration was solved through the genetic algorithm (GA), which was proposed by Holland, 1992. GA applies principles of evolution on a randomly generated sample (or population) of candidate solutions (or parent genes). These solutions are evaluated through the objective function, where nature-inspired processes such as mutation, selection and crossover enable to exploit features in the parent genes that lead to optimal solutions.

3. RESULTS

The main results from the study are included in this section, in which the outputs of the simulated model were contrasted with the measurements for the different operational periods, where the IMC, FC and FA were applied.

3.1. Initial model calibration

As shown in Figure 3, the parameters with the lowest sensitivity indicators from the Sobol and Morris methods were the desuperheater and condenser chevron angles (Φ_{DSH} and Φ_{con}), the desuperheater area correction factor (CF_{DSH}), as well as the time constants for the expansion valves' controllers ($Ti_{val,HS}$ and $Ti_{val,LS}$). Hence, these four parameters were not included for the IMC process. The Sobol and Morris sensitivity indicators revealed that the parameters with the largest influence on the variability of the CTs were related to the evaporator geometry (Φ_{eva} and CF_{eva}) and the control of the LS compressor ($Ti_{com,LS}$).

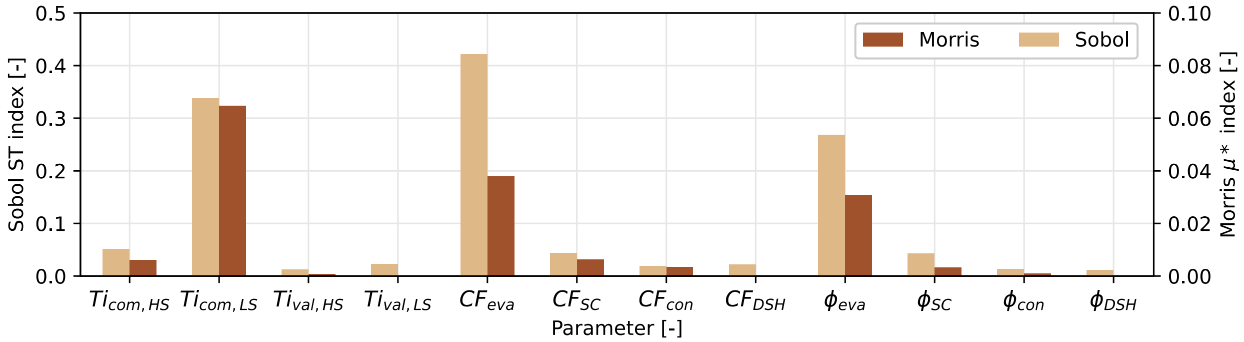

Figure 3: Sensitivity analysis results obtained from the Sobol and Morris methods

A correspondence between measured and simulated CTs was found from the IMC (see Figure 4). The simulated evaporation pressure had a lower variability compared to the measurements from this variable. This was expected because the shell-and-plate evaporator was modelled by a plate HX model, which probably did not represented in detail the dynamics of the real HX. Table 2 shows the parameters estimated through the IMC. Here, the relatively large values of $Ti_{val,HS}$ and $Ti_{val,LS}$ suggested that slow dynamics were present in the HP. It is likely that such values will be reduced if faster dynamics (e.g. start-up operation) were included in the calibration period. However, the boundary conditions in which the HP operated (e.g. sink/source temperatures and flow rates) did not vary significantly over the period monitored in this study.

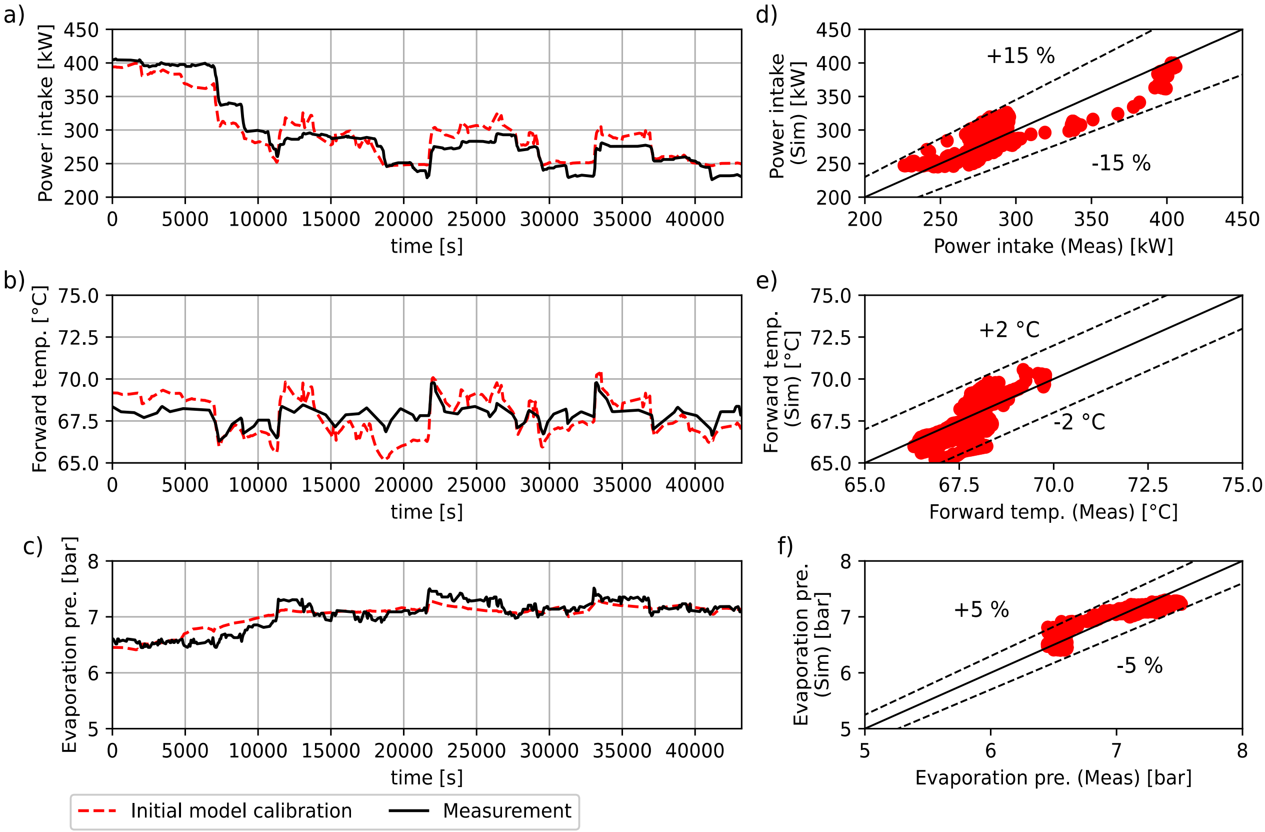

Figure 4: Calibration targets estimated in the IMC process through the GA optimization.

Table 2: Parameters from the simulation model estimated with the IMC.

Parameter	CF_{SC} [-]	Φ_{SC} [°]	CF_{con} [-]	Φ_{con} [°]	CF_{eva} [-]	Φ_{eva} [°]	$Ti_{com,HS}$ [s]	$Ti_{com,LS}$ [s]
Value	0.94	45.6	0.98	52.0	0.89	53.1	1369.6	1967.4

3.2. Fouling calibration and analysis

The results from Figure 5 showed that the FC procedure led to lower errors (up to 12 % reduction of NRMSE) compared to the IMC for variables such as COP, p_e and $\dot{W}_{total}$, particularly before the CIP was used (days A and B). For other estimated variables such as $\dot{Q}_h$, $\dot{m}_{HS}$ and $T_{sink,out}$, lower errors were obtained from the IMC than from the FC. However, the difference in terms of NRMSE when the IMC outperformed the FC was always below 2 %. The minor differences between the errors from the IMC and FC for days C and D were because the IMC was performed on a period shortly after the CIP was implemented, where fouling had a low influence on the system performance. Thereby, the calibration of fouling-related parameters in the model had a minor effect on the simulation outputs from days C and D.

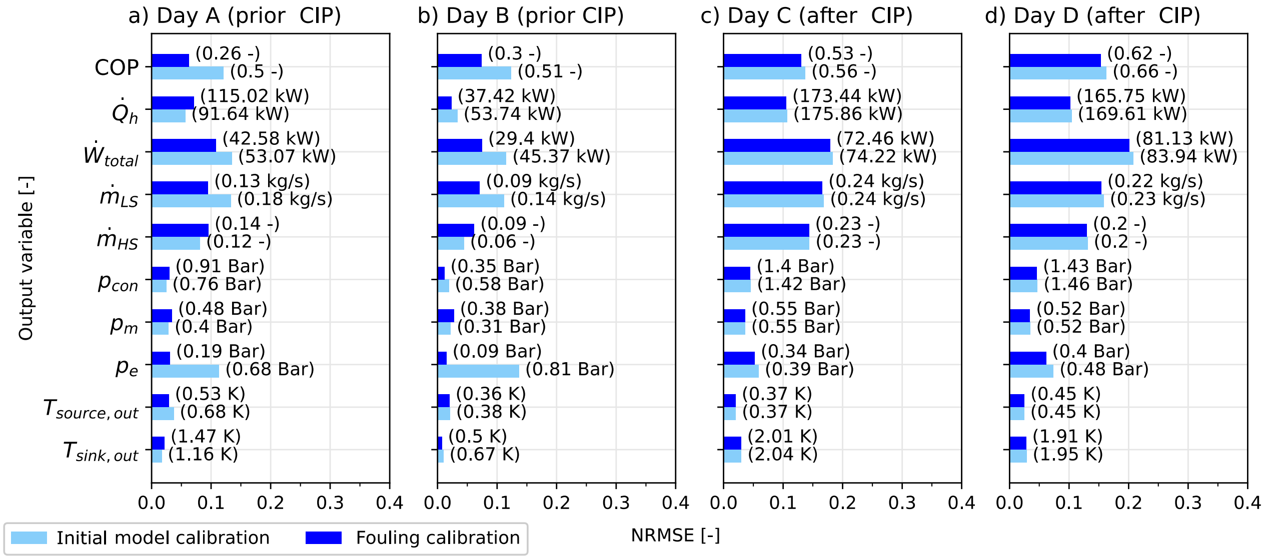

Figure 5: Simulation errors when the FC and IMC procedures were applied for the four different days of analysis, before and after the CIP was used. RMSEs are presented in ().

The FC applied on the first 12 hours of days A, B, C and D enabled the estimation of $R_{th,f}$ and dp_f on the second half of such days, shown in Figure 6. The ratio between the fouling thermal resistance and the mean thermal resistance in the evaporator ($R_{th,f}$ /$R_{th,eva}$) was significantly higher than the ratio between the fouling pressure drop and the mean pressure drop in the source stream (dp_f /dp_{eva}) for the two days prior to the CIP (days A and B). It was estimated that around 40 % of the evaporator thermal resistance was attributed to fouling before the CIP was applied. It was observed that the CIP led to a higher reduction of $R_{th,f}$ (nearly 33 %) compared to dp_f (nearly 3 %).

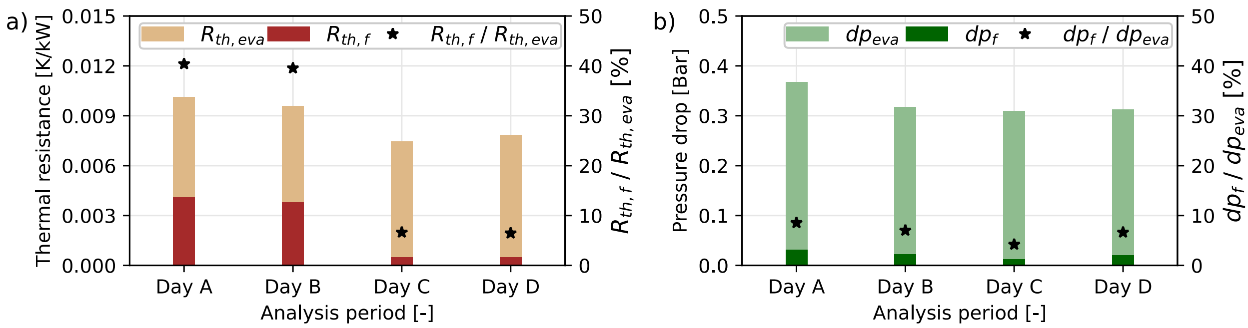

Figure 6: Fouling-related parameters estimated with the FC process.

If the CIP was used just before the periods where the effects of fouling were more extensive (i.e. days A and B), it was estimated that the COP of the HP would have increased by around 0.2 [-] due to a reduction of the total power intake, as shown in Figure 7. Here, those two days of operation were simulated considering $R_{th,f}$ and dp_f from Day C, i.e. a day of operation after the CIP was applied in the HP.

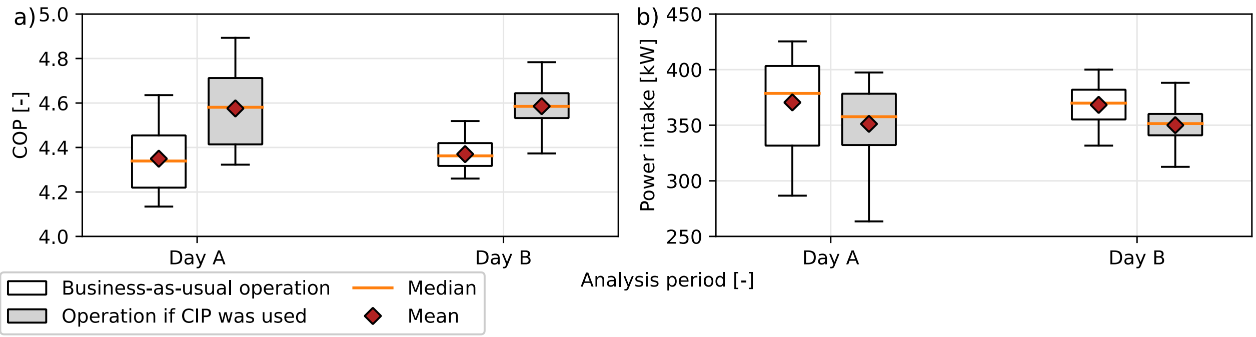

Figure 7: Simulated impact of CIP usage on the COP and total power intake during periods when the HP was most affected by fouling.

4. DISCUSSION

The proposed monitoring framework represents an inexpensive, remote, and non-intrusive approach for the assessment of the negative impacts of fouling in operational large-scale HPs. This framework does not provide a detailed characterization of fouling, where e.g. the thickness of the layer of deposited material is estimated. This can be monitored with specific sensing technologies, which include ultrasound and infrared measurements (Bott, 1995). However, such measurements are performed on-site and require specific sensing devices. The framework in this study leverages existing sensing and control systems for the estimation of fouling development over time and allows remote assessment of its impact on the HP operation. Herein, the effects of fouling on the evaporator thermal resistance and source pressure drop were characterized through a data-driven calibration method, which indicated that fouling could be better identified through the effects on the former than on the latter (see Figure 6). Moreover, such a method enabled the estimation of the HP performance given the use of CIP right before the periods with the highest levels of fouling (see Figure 7).

The calibration of fouling-related parameters led to lower simulation errors compared to the sole use of the initial model calibration for the days prior the CIP (see Figure 5). The proposed fouling calibration process enabled the reduction of the discrepancies between simulation results and measurements, which had a larger effect on periods where the influence of fouling was more extensive. A number of assumptions were included in the dynamic simulation model (e.g. omission of pressure drops in the HXs' refrigerant side, oil in the system and heat losses to the environment) and their effects on the discrepancies between simulations and measurements were likely to be lumped into the parameters selected for calibration. For instance, dynamics in the physical HP that were not included in the model were expected to be lumped in the time constants from the controllers. However, such discrepancies were probably similar for periods with and without fouling and thereby they did not prevent the calibrated model from providing useful insights about the development of fouling over time.

The analysis of fouling was based on four days of operational data, but a more extended period would be useful for the assessment of fouling growth. This may enable the provision of predictive maintenance services, as done by Meesenburg et al., 2022. Moreover, non-fouling related parameters of the dynamic model were only calibrated once in this study, but a re-calibration of such parameters over time could be performed, as implemented by Vering et al., 2021. However, it is not guaranteed that re-calibration will reduce simulation errors due to similar boundary conditions between calibration periods, model over-fitting and/or the limited capability of the model to describe the HP operation.

The proposed framework is computationally expensive and the automatic selection of calibration parameters through sensitivity analysis contributed to the reduction of the required computational time for model calibration. The use of a simpler model such as a quasi-static simulation model may lead to similar results than those from the present study. However, the use of a dynamic simulation model as the one included in this study may also enable the analysis of other faults than fouling such as refrigerant leakage, where faster dynamics may occur. In the study from Aguilera et al., 2022, a number of faults including refrigerant leakage were induced in a validated dynamic simulation model of a chiller. Here, the simulation results allowed detecting the occurrence of faults in the real system. However, evaporator fouling was the only fault identified in the HP included in the present study, which prevented the analysis of multiple faults with the same model-based framework.

Despite the possibility for automatic model calibration, the framework requires human intervention in different stages, that is, on the development of the dynamic model, the selection of periods used for the initial model calibration, the selection parameters for the sensitivity analysis, as well as the definition of the targets and their level of importance (or weights). The implementation of this framework on a different system or a significantly different operational period from the current one (e.g. on a different season) will require a human to re-evaluate the validity of model and the assumptions behind the calibration process.

5. CONCLUSIONS

A framework for monitoring a large-scale heat pump affected by evaporator fouling was developed and tested, which included a dynamic simulation model and a data-driven dynamic calibration method. A period of operation was selected for an initial calibration of the model and four different periods were used for model calibration and operational analysis given different levels of fouling growth. The results showed that the simulation errors from the model with an initial calibration decreased by up to 12 % points when the calibration also integrated fouling-related effects on the heat resistance and source pressure drop in the evaporator. The proposed framework indicated that fouling had a larger effect on the former than on the latter, which were reduced by 33 % and 3 %, respectively, with the use of cleaning-in-place. In this context, the dynamic model enabled the evaluation of the use of cleaning-in-place before periods where the heat pump was most affected by fouling.

ACKNOWLEDGEMENTS

This work was funded by EUDP (Energy Technology Development and Demonstration) under the project "Digital twins for large-scale heat pump and refrigeration systems" (project number: 64019-0570).

NOMENCLATURE

Abbreviations	
API	application programming interface
CF	area correction factor
CIP	cleaning-in-place
CT	calibration target
FA	fouling analysis
FC	fouling calibration
FMU	functional mockup unit
GA	genetic algorithm
HP	heat pump
HS	high-stage
IMC	Initial model calibration
LS	low-stage
(N)RMSE	(normalized) root mean square error

Latin symbols	
dp	pressure difference (bar)
$\dot{m}$	mass flow rate (kg/s)
$\dot{Q}$	heat flow rate (kW)
p	pressure (bar)
R	resistance (K/kW)
S	Sobol sensitivity index (-)
T	temperature (˚C)
Ti	time constant (s)
UA	overall heat transfer coefficient (kW/K)
$\dot{V}$	volume flow rate (m^3/s)
w	weight (-)
$\dot{W}$	power (kW)

Greek symbols	
μ^*	Morris mean elementary effect (-)
Φ	chevron angle (˚)

Subscripts and indices	
c	condensation
clean	clean
con	condenser
DSH	desuperheater
meas	measurement
e	evaporation
eva	evaporator
f	fouling
h	heat output
in	inlet
m	intermediate
out	outlet
sc	sub-cooler
sim	simulation
sink	sink stream
sp	set point
source	source stream
T	total sensitivity effects
total	total
th	thermal
w	water

REFERENCES

Aguilera, J. J., Meesenburg, W., Andreas, S., Ommen, T., Markussen, W. B., Zühlsdorf, B., Poulsen, J. L., Försterling, S., Elmegaard, B., 2022a. Integration of dynamic model and classification methods for fault detection and diagnosis in a chiller. Proceedings of the 15th IIR-Gustav Lorentzen Conference on Natural Refrigerants, Trondheim, Norway. IIF/IIR, 14 p.

Aguilera, J. J., Meesenburg, W., Ommen, T., Markussen, W. B., Poulsen, J. L., Zühlsdorf, B., Elmegaard, B., 2022b. A review of common faults in large-scale heat pumps. Renewable and Sustainable Energy Reviews, 168, 112826.

Bell, I. H., Wronski, J., Quoilin, S., Lemort, V., 2014. Pure and Pseudo-pure Fluid Thermophysical Property Evaluation and the Open-Source Thermophysical Property Library CoolProp.

Blank, J., Deb, K., 2020. pymoo: Multi-Objective Optimization in Python. IEEE Access, 8, 89497–89509.

Bott, T. R., 1995. Fouling of heat exchangers. Elsevier Science B.V., Amsterdam, 516 p.

Danish Energy Agency, 2022. Climate status and projection 2022 (KF22): Electricity and district heating (excluding waste incineration) (in Danish).

Dassault Systèmes, 2022. Dymola Systems Engineering. URL: https://www.3ds.com/products-services/catia/products/dymola/ (accessed 10.12.22).

Herman, J., Usher, W., 2017. SALib: An open-source Python library for sensitivity analysis. Journal of Open Source Software, 2(9), 97.

Holland, J. H., 1992. Genetic Algorithms. Scientific American, 267(1), 66–73.

IEA, 2022. The future of heat pumps. International Energy Agency (IEA), Paris, 110 p.

Kosmadakis, G., 2019. Estimating the potential of industrial (high-temperature) heat pumps for exploiting waste heat in EU industries. Applied Thermal Engineering, 156, 287–298.

Meesenburg, W., Aguilera, J. J., Kofler, R., Markussen W. B., Elmegaard, B., 2022. Prediction of fouling in sewage water heat pump for predictive maintenance. Proceedings of the 35th International Conference on Efficiency, Cost, Optimization, Simulation and Environmental Impact of Energy Systems, Copenhagen, Denmark. ECOS, 12 p.

Meesenburg, W., Kofler, R., Ommen, T., Markussen, W. B., Elmegaard, B., 2019. Design considerations for dynamically operated large-scale ammonia heat pumps. Proceedings of the 25th IIR International Congress of Refrigeration, Montréal, Canada. IIF/IIR, 2591-2598.

Pieper, H., Ommen, T., Buhler, F., Paaske, B.L., Elmegaard, B., Markussen, W. B., 2018. Allocation of investment costs for large-scale heat pumps supplying district heating. Energy Procedia, 147, 358–367.

Seifert, J., Haupt, L., Schinke, L., Perschk, A., Hackensellner, T., Wiemann, S., Knorr, M., 2022. Digital twin for heat pump systems: Description of a holistic approach consisting of numerical models and system platform. CLIMA 2022 Conference, SE-Digitization, 7.

Sommer, T., Kessler, M., Thorade, M., 2023. FMPy version 0.3.14.

TLK-Thermo GmbH, 2023. TIL Suite and TILMedia for Modelica (Version 3.12.0).

Vering, C., Borges, S., Coakley, D., Krützfeldt, H., Mehrfeld, P., Müller, D., 2021. Digital twin design with on-line calibration for HVAC systems in buildings. Proceedings of the 17th IBPSA Building Simulation Conference, Bruges, Belgium. IBPSA, 8 p.

Wüllhorst, F., Storek, T., Mehrfeld, P., Müller, D., 2022. AixCaliBuHA: Automated calibration of building and HVAC systems. Journal of Open Source Software, 7(72), 3861.

Ziegler, J.G., Nichols, N.B., 1942. Optimum settings for automatic controllers. Transactions of the American society of mechanical engineers, 64(8), 759-765.